Effects of Sulfhydryl Reagents on the Regulation of Cytosolic pH in Rat Sublingual Acini (43961)

GUO H. ZHANG*,[1] AND JAMES E. MELVIN*,†

Department of Dental Research and Neurobiology and Anatomy,† University of Rochester, Rochester, New York 14642*

Abstract. **The effects of sulfhydryl (SH) reagents on the regulation of cytosolic pH (pH_i) in rat sublingual mucous acini were examined using the pH-sensitive dye 2',7'-biscarboxyethyl-5(6)-carboxyfluorescein (BCECF). The membrane permeable SH reagent N-ethylmaleimide (NEM) resulted in a cytosolic acidification (0.19 ± 0.02 pH unit after 5-min treatment). In contrast, the impermeable SH reagents 5,5'-dithiobis(2-nitrobenzoic acid) (DTNB), p-chloromercuribenzoic acid (PCMB) and Cu^{2+} did not affect the resting pH_i. Muscarinic stimulation with carbachol (CCh) induced a cytosolic acidification (0.15 ± 0.01 pH unit after 5 min). Cu^{2+} enhanced the CCh-stimulated acidification 2-fold (0.30 ± 0.02 pH unit after 5 min). Preincubation with SH reducing agent dithiothreitol (DTT) prevented the NEM-induced and Cu^{2+}-enhanced pH_i decreases. The Cu^{2+}-enhanced but not the NEM-induced acidifications were reversed by addition of DTT after stimulation. Na^+/H^+ exchange was not influenced by Cu^{2+} or NEM, suggesting that the SH reagent–induced acidification is not caused by inhibition of exchanger activity. Anion channel inhibitor diphenylamine-2-carboxylate (DPC) abolished the NEM-induced and the Cu^{2+}-enhanced acidifications, suggesting that the acidification was mediated by HCO_3^- efflux via anion channels. Cu^{2+} did not affect the CCh-evoked increase in cytosolic free Ca^{2+} concentration ($[Ca^{2+}]_i$). In contrast, NEM triggered an elevation in $[Ca^{2+}]_i$, and DTT completely prevented this increase. The CCH-stimulated $[Ca^{2+}]_i$ increases were prevented by blocking Ca^{2+} release from the intracellular pool with 8-(diethylamino)-octyl-3,4,5-trimethoxybenzoate (TMB-8), and the NEM-stimulated $[Ca^{2+}]_i$ increases were abolished by chelating cytosolic Ca^{2+} with bis-(o-aminophenoxy)-ethane-N,N,N',N'-tetraacetic acid (BAPTA). TMB-8 prevented the CCh-stimulated, but not the Cu^{2+}-enhanced pH_i decrease, and the NEM-induced pH_i decrease was not blocked by BAPTA, suggesting that the effects of Cu^{2+} and NEM on anion channels are independent of Ca^{2+}. Taken together, these results indicate that SH groups play a critical role in pH_i regulation and the reactive SH groups are probably located on cytoplasmic site(s) of anion channels or an associated regulatory protein.**

[P.S.E.B.M. 1996, Vol 211]

The importance of sulfhydryl (SH) groups in cell transport function has been well documented. SH groups play a critical role in organic anion transport (1, 2). SH groups are essential for glucose transport (3–5) and are related to the ion permeability (6) in erythrocytes. SH groups also play a vital role in organic cation transport in renal brush-border and basolateral membranes (7, 8). It is well known that SH group modification induces rapid Ca^{2+} release from sarcoplasmic reticulum (9–12) and endoplasmic reticulum of liver cells (13). The redox reaction of SH groups regulates Ca^{2+} channel operation (14). Little is known about the effect of SH group modification on salivary fluid secretion and ion transport. In parotid cells, a reduced SH group may be essential for normal $Na^+/K^+/2Cl^-$ cotransport function and binding of the loop diuretic bumetanide (15).

According to the current fluid secretion model (16), the transepithelial movement of Cl^- is the driving

[1] To whom requests for reprints should be addressed at Department of Dental Research, University of Rochester, Box 611, 601 Elmwood Avenue, Rochester, NY 14642.

Received June 7, 1995. [P.S.E.B.M. 1996, Vol 211]
Accepted September 18, 1995.

0037-9727/96/2112-0190$10.50/0

force for fluid and electrolyte secretion in salivary glands. Cl^- efflux via an apical anion conductance pathway is accompanied by an acidification induced by HCO_3^- efflux that is apparently mediated by the same anion channel (17–22). This anion efflux pathway is regulated by modest changes in pH_i, the activity decreasing as the pH_i drops (23). In contrast, the Na^+/H^+ exchange is activated by a drop in the pH_i (71–20, 22). We have previously reported that the muscarinic-stimulated pH_i decrease observed in sublingual acini is independent of extracellular Cl^-, is inhibitable by diphenylamine-2-carboxylate (a Cl^- channel blocker), requires HCO_3^-, activates Na^+/H^+ exchange, and is dependent on intracellular Ca^{2+} indicating that the acidification is produced by Ca^{2+}-activated HCO_3^- efflux via anion channels (22). Thus, Ca^{2+} plays a critical role in pH_i regulation. Since SH reagents affect Ca^{2+} mobilization, elucidation of the influence of SH reagents on pH_i may provide important insights into the pH_i regulatory mechanisms in salivary acinar cells. In the present study we examined the effects of SH reagents on the regulation of pH_i and $[Ca^{2+}]_i$ in rat sublingual mucous acini. Our results suggest that SH reagents may modulate pH_i by enhancing HCO_3^- efflux via anion channels.

Materials and Methods

Animals. Male, 150-250-g Wistar strain rats (Charles River, Kingston Facility, NY) were used in all experiments. Rats were maintained in a room with controlled photoperiod (12:12-hr light:dark cycle) and temperature (23°C) and with standard rat (Purina 5001) chow and water available *ad libitum*.

Materials. Earle's minimal essential medium was purchased from Biofluids (Rockville, MD). *bis*(o aminophenoxy)-ethane-N,N,N′,N′-tetraacetic acid (BAPTA) and 2′,7′-*bis*(2-carboxyethyl)-5,6-carboxyfluorescein/acetoxymethyl ester (BCECF/AM), fura-2/AM, *N*-isobutyl-*N*-methylamiloride (IMA), and ionomycin were from Molecular Probes (Eugene, OR). 4-(2-Hydroxyehtyl)-1-piperazine ethansulfonate (Hepes), *N*-ethylmaleimide (NEM), hyaluronidase (type IS), *p*-chloromercuribenzoic acid (PCMB), glutathione, reduced form (GSH), bovine serum albumin, type V (BSA), DL-dithiothreitol (DTT), 5,5′-dithiobis(2-nitrobenzoic acid) (DTNB), carbamylcholine chloride (CCh) and nigericin were from Sigma (St. Louis, MO). Collagenase (type CLSPA) was from Worthington Biochemical (Freehold, NJ). Diphenylamine-2-carboxylate (DPC) was from Fluka Chemical Co. (Ronkonkoma, NY). 8-(Diethylamino)-octyl-3,4,5-trimethoxybenzoate (TMB-8) was purchased from Aldrich Chemical (Milwaukee, WI). All other chemicals were of the highest grade available.

Solutions. The digestion medium consisted of Earle's minimal medium, 1% bovine serum albumin (BSA), 100 units/ml collagenase, and 0.2 mg/ml hyaluronidase. The experiments were carried out in a physiological salt solution (PSS) containing (in mM): 110 NaCl, 25 $NaHCO_3$, 20 Hepes, 10 glucose, 5.4 KCl, 1.2 $CaCl_2$, 0.8 $MgSO_4$, 0.4 KH_2PO_4, and 0.33 NaH_2PO_4, and pH adjusted to 7.4 with NaOH after gassing with 95% O_2 and 5% CO_2 for more than 45 min. In the experiments in which cells were prepulsed with NH_4Cl, 50 mM NaCl was replaced with equimolar NH_4Cl.

Isolation of Sublingual Acini. Rat sublingual acini were isolated as previously described (22, 24, 25). Briefly, three rats were sacrificed by exsanguination after exposure to CO_2 and the sublingual glands were removed and placed in ice-cold digestion medium. The glands were injected with 0.1 ml/gland of ice-cold digestion medium, then dissected free of connective tissue and minced in the same medium. The mince was incubated in the digestion solution at 37°C with continuous gassing (95% O_2/5% CO_2) and shaking (80 cycles/min). The mince was dispersed by gently pipetting 10 times with a 10-ml plastic pipette at 15-min intervals. After 45 min of digestion, the preparation was centrifuged at 50*g* for 30 sec and the supernatant was discarded. The preparation was resuspended in 10 ml of the fresh digestion medium and incubated for another 45 min. After 1.5 hr of digestion, the acini were washed three times with PSS containing 0.01% BSA. The resulting preparation was separated into two fractions: small (supernatant) and large aggregates by centrifugation at 400*g* for 15 sec. The small aggregates consisting of 3–10 acini were used.

Determination of Cytosolic pH. Isolated sublingual acini were loaded with the pH-sensitive fluorescent indicator, BCECF, and the cytosolic pH was determined as described previously (22, 25). The acini were incubated in PSS containing 0.01% BSA and 2 μ*M* BCECF/AM at 23°C for 30 min. After loading, the acini were rinsed twice by centrifugation at 50*g* for 30 sec and resuspended in PSS containing 0.01% BSA. The BCECF-loaded acini were continuously agitated and gassed with 95% O_2 and 5% CO_2 at 23°C until use. An aliquot of BCECF-loaded acini was centrifuged at 400*g* for 15 sec and resuspended in BSA-free PSS to promote attachment and added to a coverslip mounted in a perfusion chamber on a Nikon inverted microscope interfaced to a SPEX AR CM fluorometer (Edison, NJ). The perfusion system consisted of reservoirs connected to the perfusion chamber via polyethylene tubing. During pH determination, solutions were gassed continuously with 95% O_2 and 5% CO_2. The perfusion rate was 4 ml/min and the turnover time of solution in the chamber was less than 5 sec. A pinhole turret was used to focus on five to eight cells with a Nikon Fluor 40X 1.3-NA oil immersion objective. The BCECF fluorescence was continuously monitored by

alternating the excitation wavelength between 500 and 440 nm and collecting the emission at 530 nm. The pH value was calculated using an *in situ* calibration technique (26). Briefly, the acini were superfused with a series of HEPES-buffered high K^+ solutions containing 120 m*M* KCl, 20 m*M* NaCl, 20 m*M* HEPES, 0.8 m*M* $MgCl_2$, and 5 μ*M* nigericin at different pHs (6.8–7.6). In this pH range, the 500/440 nm fluorescence ratio was linearly related to the cytosolic pH. An acute acid loading was produced by the NH_4^+/NH_3 prepulse technique described by Roos and Boron (27). BCECF-loaded acini were exposed to an acid-loading PSS in which 50 m*M* NaCl was substituted with 50 m*M* NH_4Cl.

Determination of Cytosolic Free [Ca^{2+}]. The cytosolic free Ca^{2+} concentration ($[Ca^{2+}]_i$) was determined using the Ca^{2+}-sensitive dye fura-2 as previously described (24, 28, 29). Briefly, sublingual mucous acini were loaded with 2 μ*M* fura-2/AM by incubating at 23°C for 30 min. Fura-2–loaded acini were rinsed twice with PSS containing 0.01% BSA and resuspended in the same medium. A 0.5-ml aliquot of fura-2–loaded acini was centrifuged, resuspended in PSS without BSA, and placed in the perfusion chamber. The excitation wavelengths were 340 nm and 380 nm, and the emission wavelength was 505 nm. Calibration of the $[Ca^{2+}]_i$ was performed *in situ* as previously described (24, 28, 29). Cytosolic free $[Ca^{2+}]$ was then calculated according to Grynkiewicz *et al.* (30) using 224 n*M* as the K_d of fura-2 for Ca^{2+}.

Determination of Fura-2 Fluorescence Quenching by Cu^{2+}. Fura-2 fluorescence quenching by Cu^{2+} was monitored as previously described for Mn^{2+} (25, 28–31). Cu^{2+} quenches the fluorescence of fura-2, thus a decrease in fluorescence reflects Cu^{2+} influx. Fura-2–loaded acini were superfused with a Ca^{2+}-free PSS. The Ca^{2+}-insensitive wavelength 360 nm and an emission wavelength of 505 nm were used to monitor the fluorescence change. Fura-2 fluorescence quenching by Cu^{2+} is expressed as percentage per minute.

Data Analysis and Statistics. The magnitude of the pH_i change was determined at 5 min after stimulation and expressed as pH unit after 5 min. Initial rates were determined using the 1st-min pH_i changes, when the rate of change was relatively linear, and expressed as pH unit/per minute. All results are presented as means ± SEM of at least four determinations using different cell preparations. Comparisons were made using the unpaired Student's *t* test.

Results

SH Reagent–induced Cytosolic Acidification. SH reagents were used to test the effect of SH group modification on pH_i. DTNB (1 m*M*), a membrane impermeable SH reagent (32,33), PCMB (0.1 m*M*), a slowly permeable SH reagent (34, 35) or Cu^{2+} (0.1 m*M*) did not influence resting pH_i in sublingual acini in 5–6 min (Fig. 1A). However, the permeable SH reagent NEM (36) (1 m*M*) induced a pH_i decrease (0.19 ± 0.02 pH unit after 5 min, initial rate 0.11 ± 0.01 pH unit/min, $n = 5$). These results indicate that acute SH group modification of extracellular sites is not involved in pH_i regulation. Stimulation of acini with 10 μ*M* CCh resulted in a cytosolic acidification (0.15 ± 0.01 pH unit after 5 min, $n = 11$) as previously reported (22, 25). Cu^{2+} significantly potentiated the CCh-induced acidification (0.30 ± 0.02 pH unit after 5 min, $n = 6$; $P < 0.001$; Fig. 1B). Stimulation in the presence of PCMB, however, did not potentiate the CCh-induced acidification (0.14 ± 0.03 pH unit after 5 min, $n = 4$), possibly suggesting that the reactive SH groups are located on the cytoplasmic side of the plasma membrane.

Since Cu^{2+} did not induce pH_i change in the absence of CCh-stimulation, it is postulated that the Cu^{2+} permeability increased during stimulation. Cu^{2+} influx was monitored by measuring the quenching by Cu^{2+} of fura-2 fluorescence. As shown in Figure 2, Cu^{2+} did not quench fura-2 fluorescence under resting conditions (0.3 ± 0.3%/min, $n = 5$); however, CCh stimulation induced a significant quenching (5.6 ± 0.9%/min, $n = 6$; $P < 0.001$), suggesting that muscarinic stimulation activates Cu^{2+} entry.

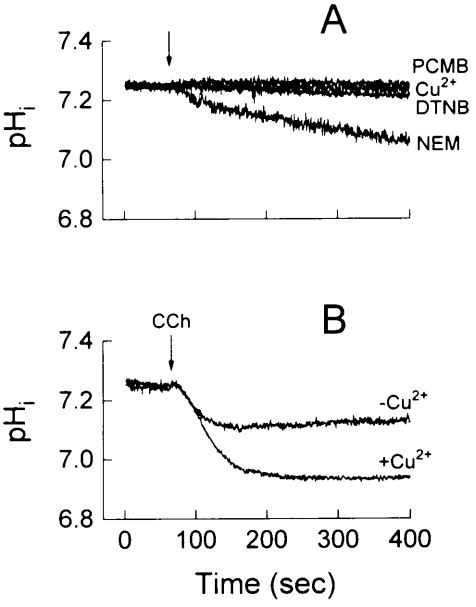

Figure 1. Effects of DTNB, PCMB, NEM, and Cu^{2+} on pH_i in rat sublingual mucous acini. 2',7'-Biscarboxyethyl-5(6)-carboxyfluorescein (BCECF)–loaded rat sublingual acini were superfused with a physiological salt solution (PSS). Treatments were applied at the time indicated by the arrows. The traces are representatives of at least four experiments using different cell preparations (A). BCECF-loaded acini were treated with 1 m*M* 5,5'-dithiobis(2-nitrobenzoic acid) (DTNB, $n = 5$), 100 μ*M* p-chloromercuribenzoic acid (PCMB, $n = 4$), 100 μ*M* $CuSO_4$ ($n = 4$), or 1 m*M* N-ethylmaleimide (NEM, $n = 5$); (B) BCECF-loaded acini were stimulated with 10 μ*M* carbachol (CCh) either in the absence ($-Cu^{2+}$, $n = 11$) or presence ($+Cu^{2+}$, $n = 6$) of 100 μ*M* $CuSO_4$.

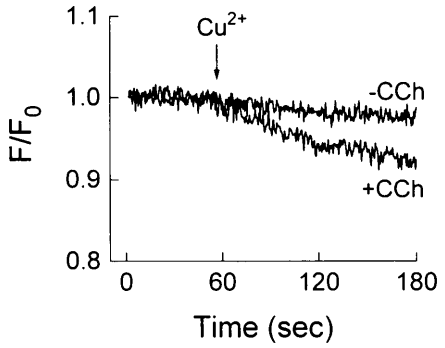

Figure 2. Quenching of fura-2 fluorescence by Cu^{2+} influx. Fura-2–loaded acini were superfused with a Ca^{2+}-free physiological salt solution and fluorescence was determined at the Ca^{2+}-insensitive excitation wavelength (360 nm). In the muscarinic stimulation experiments, acini were treated with 10 μM CCh (+CCh, $n = 6$). Control experiments were performed in the same fashion but the same volume of water was added (−CCh, $n = 5$). Cu^{2+} (0.1 mM) was added to initiate fura-2 quenching at 2 min following the muscarinic or control treatment.

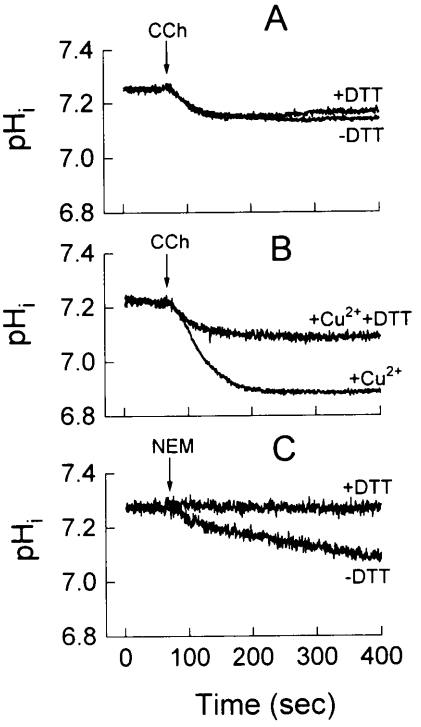

Figure 3. Protective effects of DTT on CCh-induced, NEM-induced, or Cu^{2+}-enhanced acidification. (A) BCECF-loaded acini were stimulated with 10 μM CCh in the absence (−DTT, $n = 11$) or presence (+DTT, $n = 5$) of 1 mM dithiothreitol. (B) BCECF-loaded acini were superfused with PSS containing 0.1 mM Cu^{2+}, then stimulated with 10 μM CCh in the absence (+Cu^{2+}, $n = 6$) or presence (Cu^{2+} +DTT, $n = 4$) of 1 mM DTT. (C) BCECF-loaded acini were superfused with PSS and stimulated with 1 mM NEM in the absence (−DTT, $n = 5$) or presence (+DTT, $n = 4$) of 1 mM DTT.

To confirm that the effects of NEM and Cu^{2+} were by reaction with SH groups and that the reactive SH groups are located at the cytoplasmic face of the plasma membrane, the protective effect of SH group reducing agents was tested. The membrane permeable SH reducing agent DTT (1 mM) did not significantly change the CCh-stimulated acidification (0.13 ± 0.01 pH unit after 5 min, $n = 5$; Fig. 3A), but inhibited both the Cu^{2+}-enhanced (0.09 ± 0.03 pH unit after 5 min, $n = 4$; Fig. 3B) and the NEM-induced (0.01 ± 0.01 pH unit after 5 min, $n = 4$; Fig. 3C) acidifications. Application of DTT after the Cu^{2+}-enhanced acidification reversed the pH_i (pH_i recovery 0.18 ± 0.02 unit, $n = 4$), but the relatively impermeable reducing agent, the reduced form of glutathione (GSH), was much less effective (pH_i recovery 0.04 ± 0.01 pH unit, $n = 4$; $P < 0.001$; Fig. 4A), suggesting that the reactive SH groups are located inside the plasma membrane. Addition of 2 mM DTT *after* NEM did not reverse the acidification (pH_i decrease 0.20 ± 0.04 pH unit after 5 min, $n = 7$; Fig. 4B) consistent with the irreversible nature of the NEM reaction (35).

Effect of SH Reagents on Na^+/H^+ Exchange. In sublingual mucous acini during stimulation, pH_i is primarily regulated by two ion transport mechanisms, HCO_3^- efflux via the Ca^{2+}-activated apical anion channels, which induces a cytosolic acidification, and proton extrusion mediated by the Na^+/H^+ exchanger in the basolateral membrane, which buffers the pH_i decrease (22). The SH reagent-induced acidification is therefore most likely mediated by activation of HCO_3^- efflux and/or inhibition of Na^+/H^+ exchange. To further elucidate the mechanism by which SH reagents induce cytosolic acidification, the influence of Cu^{2+} and NEM on Na^+/H^+ exchange was tested. BCECF-loaded acini were exposed to an acute acid-load using the NH_4^+/NH_3 prepulse technique (22, 25, 27). The pH_i recovery following this acid load is mediated by Na^+/H^+ exchange in sublingual acini (22). As shown in Fig. 5A, pH_i rapidly recovered after the NH_4^+/NH_3 prepulse (initial recovery rate 0.21 ± 0.04 pH unit/min, $n = 6$). Cu^{2+} and DTT did not significantly inhibit the pH_i recovery rate (Cu^{2+}: 0.15 ± 0.02 pH unit/min, $n = 5$; $P > 0.05$; Cu^{2+} +DTT: 0.16 ± 0.01 pH unit/min, $n = 5$; $P > 0.05$; Fig. 5B). However, the initial pH_i recovery rate (0.08 ± 0.03 pH unit/min, $n = 5$; Fig. 5C) in the presence of 1 mM NEM was significantly smaller (<40%, $P < 0.05$) than control. DTT (2 mM) completely prevented the inhibition by NEM (0.22 ± 0.02 pH unit/min, $n = 4$; Fig. 5C). Considering the rate of NEM-induced acidification (0.11 ± 0.01 pH unit/min, Fig. 1B), the reduced pH_i recovery in the presence of NEM may be related to increased Ca^{2+}-activated HCO_3^- efflux (acidification).

Effect of SH Reagents on HCO_3^- Efflux via the Apical Anion Channels. The muscarinic-stimulated acidification in sublingual cells is mediated by HCO_3^- efflux via anion channels (22). To clarify which mechanism is responsible for the SH reagent–induced acidification, a Na^+/H^+ exchange inhibitor, IMA was

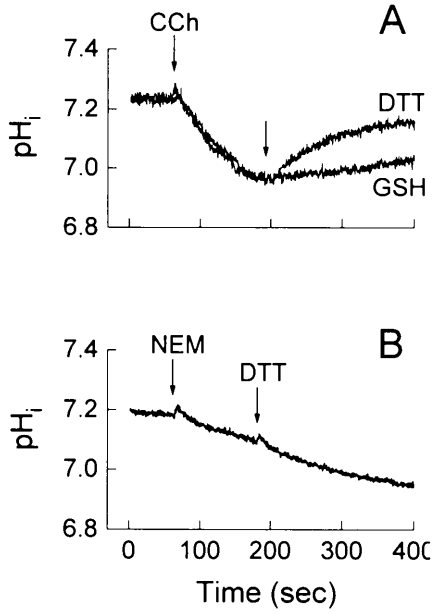

Figure 4. The pH_i recovery induced by DTT and GSH after the NEM-induced or Cu^{2+}-enhanced acidification. BCECF-loaded acini were superfused as described in Figure 1. (A) pH_i recovery by DTT or GSH after the Cu^{2+}-enhanced acidification. At the time indicated by the first arrow, 0.1 m*M* $CuSO_4$ and 10 μ*M* carbachol were added. Two minutes later, at the time indicated by the second arrow, 1 m*M* DTT (DTT, $n = 4$) or 2 m*M* glutathione (GSH, reduced form, $n = 5$) was added. (B) Effect of DTT on pH_i during the NEM-induced acidification. At the time indicated by the arrows, 1 m*M* NEM and 2 m*M* DTT were added ($n = 7$).

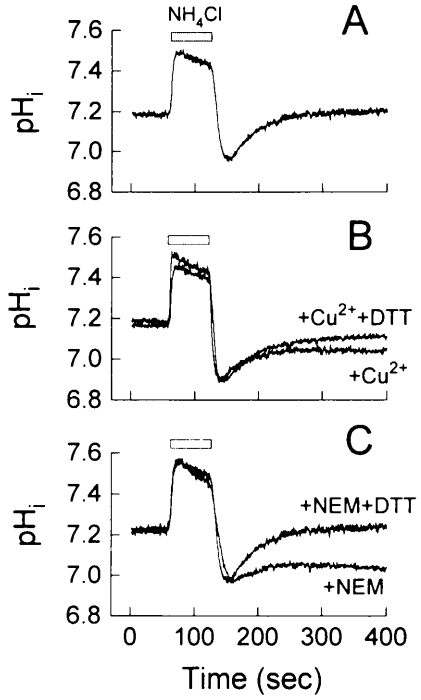

Figure 5. Effects of NEM and Cu^{2+} on Na^+/H^+ exchange: protection by DTT. BCECF-loaded sublingual acini were superfused as described in Figure 1. At the time indicated by the bar, acini were exposed to a 50 m*M* NH_4Cl prepulse for 60 sec. (A) After the prepulse, acini were superfused with PSS ($n = 6$); (B) After the prepulse, acini were superfused with PSS containing 0.1 m*M* Cu^{2+} ($+Cu^{2+}$, $n = 5$) or 0.1 m*M* Cu^{2+} and 1 m*M* DTT ($+Cu^{2+}+DTT$, $n = 5$); (C) Acini were prepulsed with 50 m*M* NH_4Cl in PSS, then superfused with PSS containing 1 m*M* NEM ($+NEM$, $n = 5$), or 1 m*M* NEM and 1 m*M* DTT ($+NEM+DTT$, $n = 4$). The pH recovery rate was calculated using the linear portion of the pH change (first 30 sec).

used to block pH_i recovery. IMA inhibits Na^+/H^+ exchange with a K_i of 0.4 μ*M* in rat sublingual acinar cells (22); thus, in the presence of 25 μ*M* IMA, the agonist-induced pH_i decrease reflects HCO_3^- efflux. As shown in Table I, the CCh-stimulated acidification dramatically increased in the presence of IMA ($+IMA$) or Cu^{2+} ($+Cu^{2+}$). The resulting IMA-induced *net* pH_i decrease was: 0.22 units; while, the Cu^{2+}-induced *net* pH_i decrease was 0.15 pH unit after 5 min (the difference between CCh and $+Cu^{2+}$). In the presence of both Cu^{2+} and IMA, the pH_i change increased further. The IMA-induced *net* pH_i decrease in the presence of Cu^{2+} (the difference between $+Cu^{2+}$ and $+Cu^{2+}+IMA$) was 0.23 pH units; whereas, the Cu^{2+}-induced *net* pH_i decrease in the presence of IMA was 0.16 pH unit after 5 min. The effects of these agents on the stimulated pH_i decrease were additive, indicating that Cu^{2+} and IMA act on two separate mechanisms. Taken together, the above results support that the Cu^{2+}-enhanced acidification is derived from potentiated HCO_3^- efflux via the anion channels.

In the presence of IMA, NEM induced a larger acidification (0.29 ± 0.02 pH units after 5 min, $n = 4$, $P < 0.01$; Table I). However, the initial rate of the pH_i decrease was not altered by IMA (0.12 ± 0.03 pH unit/min, $n = 4$; $P > 0.05$).

To confirm that SH reagents increase HCO_3^- efflux via apical anion channels, an anion channel blocker DPC was applied to inhibit HCO_3^- efflux. As shown in Fig. 6A, 1 m*M* DPC prevented the CCh-induced acidification, as reported previously (22). DPC also dramatically inhibited the Cu^{2+}-enhanced (0.03 ± 0.01 pH unit after 5 min, $n = 4$; $P < 0.001$; Fig. 6B) and the NEM-induced (0.02 ± 0.01 pH unit after 5 min, $n = 4$; $P < 0.001$; Fig. 6C) acidifications (compare to Fig. 1), indicating that the SH reagent–induced acidification is mediated by increased HCO_3^- efflux via apical anion channels.

Effect of SH Reagents on the Intracellular Free Ca^{2+} Concentration ($[Ca^{2+}]_i$). It has been documented that anion channels are activated by Ca^{2+} in salivary acinar cells (22, 36–38). SH group modification triggers a rapid Ca^{2+} release from sarcoplasmic reticulum (9–12) and endoplasmic reticulum (13). To clarify whether the SH reagent–induced increase in HCO_3^--efflux is mediated by increasing $[Ca^{2+}]_i$, the effect of Cu^{2+} and NEM on $[Ca^{2+}]_i$ was examined using fura-2-loaded sublingual acini. Muscarinic stimulation (10 μM CCh) resulted in a 5.4-fold initial rapid

Table I. Effects of IMA on the CCh-Induced, Cu^{2+}-Enhanced, and NEM-Induced Cytosolic Acidification

Treatment	*n*	pH_i change (pH unit after 5 min)	IMA-Induced net pH_i change	Cu^{2+}-induced net pH_i change
CCh	11	0.15 ± 0.01	—	—
CCh + IMA	10	0.37 ± 0.04*	0.22[a]	—
CCh + Cu^{2+}	6	0.30 ± 0.02*	—	0.15[b]
CCh + IMA + Cu^{2+}	6	0.53 ± 0.06*†	0.23[c]	0.16[d]
NEM	5	0.19 ± 0.02	—	—
NEM + IMA	4	0.29 ± 0.02‡	0.10[e]	—

Note. BCECF-loaded acini were superfused with physiological salt solution (PSS) or PSS containing either 0.1 m*M* Cu^{2+} (+Cu^{2+}), 25 μ*M* IMA (+IMA), or both (+IMA + Cu^{2+}). Two minutes later, the acini were stimulated with 10 μ*M* carbachol (CCh) or 1 m*M* NEM. The values of the net pH changes are: [a]difference between CCh + IMA and CCh only; [b]difference between CCh + Cu^{2+} and CCh only; [c]difference between CCh + IMA + Cu^{2+} and CCh + Cu^{2+}; [d]difference between CCh + IMA + Cu^{2+} and CCh + IMA; [e]difference between NEM + IMA and NEM only.
* Value is significantly different from CCh only, $P < 0.01$.
† Value is significantly different from CCh + IMA, $P < 0.01$.
‡Value is significantly different from NEM only, $P < 0.01$.

increase in $[Ca^{2+}]_i$ (from 50.8 ± 5.8 n*M* to 273.9 ± 15.0 n*M*, $n = 12$), followed by a 3.9-fold sustained increase (199.0 ± 14.1 n*M*, $n = 12$; Fig. 7A). Cu^{2+} (0.1 mM) did not significantly alter the CCh-stimulated $[Ca^{2+}]_i$ increase (initial 261.7 ± 23.7 n*M*; sustained 174.3 ± 45.7 n*M*, $n = 4$; Fig. 7A).

The $[Ca^{2+}]_i$ increase stimulated by CCh is blocked by TMB-8, an inhibitor of Ca^{2+} release from the intracellular store (28, 39). In the present study, TMB-8 almost completely inhibited the CCh-stimulated $[Ca^{2+}]_i$ increase in the absence (initial: 63.3 ± 4.4 n*M*, sustained: 58.6 ± 1.5 n*M*, $n = 10$) and presence (initial: 86.8 ± 10.5 n*M*, sustained: 63.7 ± 8.9 n*M*, $n = 5$) of Cu^{2+} (Fig. 7A). NEM induced a slow increase in $[Ca^{2+}]_i$ (233.5 ± 12.1 n*M* after 5 min, $n = 4$; Fig. 7B)

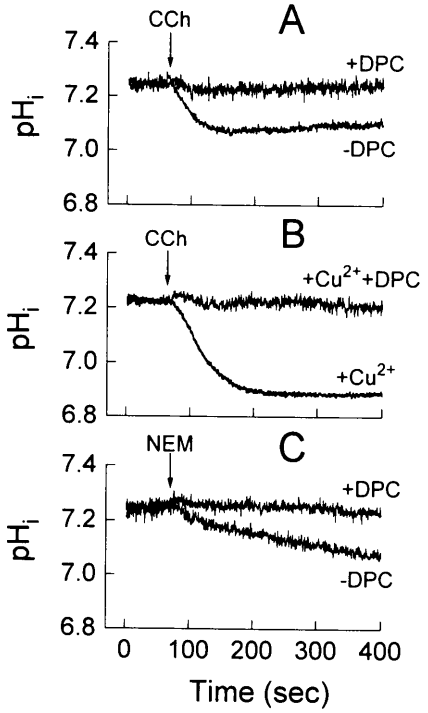

Figure 6. Inhibition by DPC of the CCh-induced, Cu^{2+}-enhanced, and NEM-induced acidification. (A) BCECF-loaded acini were superfused with PSS for 2 min, then stimulated with 10 μ*M* CCh in the absence (−DPC, $n = 11$) or presence (+DPC, $n = 6$) of 1 m*M* diphenylamine-2-carboxylate (DPC). (B) BCECF-loaded acini were superfused with PSS containing 0.1 m*M* $CuSO_4$ for 2 min, then stimulated with 10 μ*M* CCh in the absence (+Cu^{2+}, −DPC, $n = 11$) or presence (+Cu^{2+}, +DPC, $n = 4$) of 1 m*M* DPC. (C) BCECF-loaded acini were stimulated with 1 m*M* NEM in the absence (−DPC, $n = 5$) or presence (+DPC, $n = 4$) of 1 m*M* DPC.

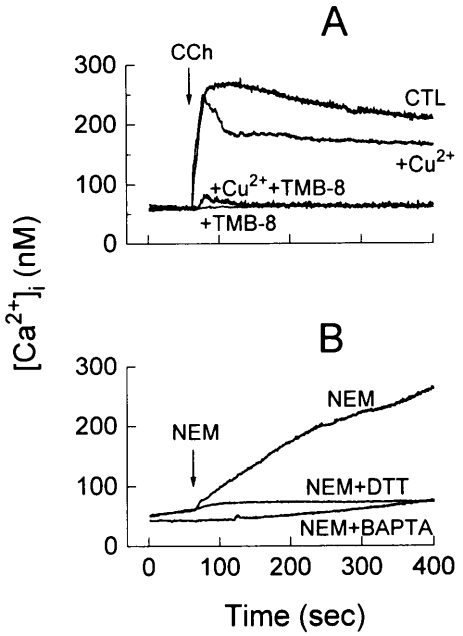

Figure 7. Effects of NEM, Cu^{2+}, TMB-8, and BAPTA on cytosolic free Ca^{2+} concentration. Rat sublingual acini were loaded with 2 μ*M* fura-2/AM for 30 min. The fura-2–loaded acini were superfused with PSS. (A) Fura-2–loaded acini were stimulated with 10 μ*M* CCh in the absence (Control, $n = 12$) or presence (Cu^{2+}, $n = 4$) of 0.1 m*M* Cu^{2+}; or acini were superfused with PSS containing 50 μ*M* TMB-8 and stimulated with CCh in the absence (TMB-8, $n = 4$) or presence (Cu^{2+} + TMB-8, $n = 5$) of 0.1 m*M* Cu^{2+}. (B) Fura-2–loaded acini were stimulated with 1 m*M* NEM in the absence (NEM, $n = 4$) or presence (NEM + DTT, $n = 5$) of 1 m*M* DTT, or the BAPTA-loaded acini (incubation with 50 μ*M* BAPTA/AM for 40 min at room temperature) were stimulated with the 1 m*M* NEM (NEM + BAPTA, $n = 5$).

of similar magnitude compared to the CCh-stimulated $[Ca^{2+}]_i$ increase. Preincubation of the cells with DTT (1 m*M*) prevented the NEM-induced $[Ca^{2+}]_i$ increase (74.7 ± 7.3 n*M* at 5 min, $n = 5$; $P < 0.001$; Fig. 7B). Loading cells with the specific Ca^{2+} chelator, BAPTA (50 μ*M*) dramatically inhibited the NEM-induced $[Ca^{2+}]_i$ increase (72.2 ± 11.0 n*M* at 5 min, $n = 5$; $P < 0.001$; Fig. 7B).

TMB-8 prevented the CCh-induced acidification (0.03 ± 0.02 pH unit/5 min, $n = 5$; Fig. 8A). In contrast, stimulation with CCh in the presence of Cu^{2+} with TMB-8 induced an acidification (0.13 ± 0.02 pH unit after 5 min, $n = 5$; $P < 0.005$; Fig. 8A). Although BAPTA inhibited the NEM-induced $[Ca^{2+}]_i$ increase, it did not prevent the NEM-induced acidification (0.10 ± 0.02 pH unit after 5 min, $n = 6$; Fig. 8B; see Fig. 1). These results suggest that SH reagents act independent of $[Ca^{2+}]_i$ on the HCO_3^- efflux pathway.

Discussion

SH groups play a critical role in biological membrane structure and function (35). Modification of these groups induces physiological and pharmacological alterations (35). SH reagents serve as useful tools for testing the functions of SH groups. In the present study we demonstrated that SH groups are essential for the regulation of intracellular pH. This is documented by: (i) the SH reagent NEM induced a significant cytosolic acidification; (ii) Cu^{2+} enhanced the muscarinic stimulation-induced acidification; and (iii) the SH group reducing agent, DTT, prevented the NEM-induced, and reversed the Cu^{2+}-enhanced acidifications.

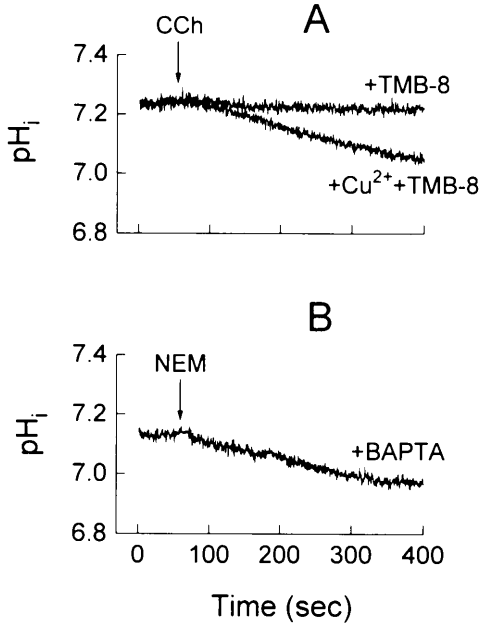

Figure 8. Effects of TMB-8 and BAPTA on Cu^{2+}-enhanced and NEM-induced intracellular acidification. Rat sublingual acini were loaded with BCECF as described in Figure 1 and with BAPTA as in Figure 7. (A) BCECF-loaded acini were superfused with PSS containing 50 μ*M* TMB-8 and stimulated with 10 μ*M* CCh in the absence (+TMB-8, $n = 5$) or presence (+TMB+Cu^{2+}, $n = 5$) of 0.1 m*M* Cu^{2+}. (B) BCECF- and BAPTA-loaded acini were stimulated with 1 m*M* NEM (+BAPTA, $n = 6$).

The results in the present study suggest that the reactive SH groups responsible for the acidification are located on the cytoplasmic surface of the plasma membrane. First, NEM, an irreversible, membrane permeable SH reagent (35, 40), produced a slow cytosolic acidification after addition. NEM covalently modifies both exofacial and endofacial SH groups of biological membranes. Because the impermeable SH reagent DTNB (32, 33) and the relatively less permeable SH reagent PCMB (34, 35) did not produce any pH_i changes (Fig. 1), even during CCh-stimulation, the reactive SH groups are most likely located inside the plasma membrane. Second, little Cu^{2+} enters cells under resting conditions (Fig. 2), therefore, like DTNB and PCMB, Cu^{2+} did not have any effect on the resting pH_i. However, during muscarinic stimulation, Cu^{2+} entered cells (Fig. 2) inducing a significant potentiation of the muscarinic-stimulated acidification. The mechanism by which Cu^{2+} influx occurs is unknown, however, Cu^{2+} may enter via a cation entry pathway. Third, DTT completely reversed the Cu^{2+}-enhanced pH acidification during stimulation, but GSH, an impermeable reducing agent (41) was not effective (Fig. 4). Taken together, these results suggest that the reactive SH groups are probably located on the cytoplasmic face of the plasma membrane.

DTT does not alter the muscarinic-stimulated acidification, suggesting that SH groups are not involved in the muscarinic-stimulated anion channel opening. Apparently, the SH groups involved are maintained in the reduced form under physiological conditions.

Since the muscarinic-induced acidification is produced by HCO_3^- efflux via anion channels and the pH_i recovery is mediated by the Na^+/H^+ exchanger in rat sublingual acini (22), the SH reagent–induced acidification may be mediated by activation of anion channels and/or by decreased Na^+/H^+ exchange. In the presence of 25 μ*M* IMA, which completely inhibits Na^+/H^+ exchange in sublingual acini (22), the magnitude of the Cu^{2+}-enhanced pH_i drop was unchanged (i.e., the effects of IMA and Cu^{2+} were additive), suggesting that the Na^+/H^+ exchanger is not involved in the Cu^{2+}-induced acidification. Therefore, it is postulated that the potentiation of the pH_i decrease by Cu^{2+} was mediated by modifying the intercellular SH group(s) of anion channels or an associated regulatory protein. Consistent with this hypothesis, the anion channel blocker DPC blocked the effects of Cu^{2+} and NEM.

The effects of the anion channel blocker, DPC,

provide evidence that Cu^{2+} and NEM primarily induce an acidification by increasing HCO_3^- efflux. DPC dramatically inhibited the NEM-induced and the Cu^{2+}-enhanced acidifications, strongly suggesting that the SH reagent–induced acidification is mediated by HCO_3^- efflux via anion channels. It appears that SH reagents bind to reactive SH groups of the anion channels (or an associated regulatory protein) and increase the probability of channel opening or single channel conductance.

Under physiological conditions, HCO_3^- efflux via the anion channels is activated by Ca^{2+} in salivary gland acinar cells (36–38) including sublingual acinar cells (22, 24, 25). SH group modification induces Ca^{2+} release from intracellular pools (9–13). Elucidation of the relationship between SH reagent–induced Ca^{2+} mobilization and pH_i is important for clarifying the mechanisms underlying the SH group modification-induced cytosolic acidification. Cu^{2+} did not alter the muscarinic stimulation-induced $[Ca^{2+}]_i$ increase, but markedly potentiated the CCh-induced acidification. SH group reducing agent DTT completely prevented the Cu^{2+}-enhanced acidification. Furthermore, using TMB-8 to prevent Ca^{2+} release from Ca^{2+} stores did not inhibit Cu^{2+} enhanced acidification (Fig. 8A), suggesting that the mechanism of the effect of Cu^{2+} on pH_i may be mediated by the interaction of Cu^{2+} with SH groups necessary for the activation of anion channels. Another SH reagent, NEM, induced a large increase in $[Ca^{2+}]_i$, however, when this $[Ca^{2+}]_i$ increase was prevented by BAPTA, the NEM-induced pH_i decrease was partly blunted (47%), suggesting that the NEM-induced acidification is mediated by both the increase in $[Ca^{2+}]_i$ and a direct interaction with SH groups involved in the activation of anion channels.

In summary, this study demonstrates that SH reagents induce an intracellular acidification that is mediated by potentiating anion channel activity by reacting with SH group(s) located inside of the plasma membrane. These results suggest that the reducing state of SH groups is important for normal channel function.

We thank Drs. William Bowen and Odette Aguirre for helpful comments. This work was supported in part by National Institutes of Health Grant DE1 1549 (J.E.M.) and STRC Grant 381 (G.H.Z.).

1. Spector R. Riboflavin transport by rabbit kidney slices: Characterization and relation to cyclic organic acid transport. J Pharmacol Exp Ther **221**:394–398, 1982.
2. Tse SS, Bildstein CL, Liu D, Mamelok RD. Effects of divalent cations and sulfhydryl reagents on the p-aminohippurate (PAH) transporter of renal basal-lateral membranes. J Pharmacol Exp Ther **226**:19–26, 1983.
3. Smith RPP, Ellman L. A study of the dependence of the human erythrocytes glucose transport system on membrane sulfhydryl groups. J Membrane Biol **12**:177–188, 1973.
4. Roberts SJ, Tanner JA, Denton RM. Properties of N-maleoylmethionine sulphone, a novel impermeant maleimide, and its use in the selective labelling of the erythrocyte glucose-transport system. Biochem J **205**:139–145, 1982.
5. Krupka RM. Reaction of the glucose carrier of erythrocytes with sodium tetrathionate: Evidence for inward-facing and outward-facing carrier conformations. J Membrane Biol **84**:35–43, 1985.
6. Knauf PA, Rothstein A. Chemical modification of membranes. I. Effects of sulfhydryl and amino reactive reagents on amino and cation permeability of the human red blood cell. J Gen Physiol **58**:190–221, 1971.
7. Sokol PP, Holohan PD, Ross CR. Essential disulfide and sulfhydryl groups for organic cation transport in renal brush-border membranes. J Biol Chem **261**:3282–3287, 1986.
8. Zimmerman WB, Byun E, McKinney TD, Sokol PP. Sulfhydryl groups are essential for organic cation exchange in rabbit renal basolateral membrane vesicles. J Biol Chem **266**:5459–5546, 1991.
9. Abramson JJ, Trimm JL, Weden L, Salama G. Heavy metals induce rapid calcium release from sarcoplasmic reticulum vesicles isolated from skeletal muscle. Proc Natl Acad Sci USA **80**:1526–1530, 1983.
10. Abramson JJ, Cronin JR, Salama G. Oxidation induced by phthalocyanine dyes causes rapid calcium release from sarcoplasmic reticulum vesicles. Arch Biochem Biophys **263**:245–255, 1988.
11. Trimm JL, Salama G, Abramson JJ. Sulfhydryl oxidation induces rapid calcium release from sarcoplasmic reticulum vesicles. J Biol Chem **261**:16092–16098, 1986.
12. Stuart J, Abramson JJ. Adenine nucleotides stimulate oxidation-induced calcium efflux from sarcoplasmic reticulum vesicles. Arch Biochem Biophys **264**:125–134, 1988.
13. Zhang GH, Yamaguchi M, Kimura S, Higham S, Kraus-Friedmann N. Effects of heavy metal on rat liver microsomal Ca^{2+}-ATPase and Ca^{2+} sequestering. Relation to SH groups. J Biol Chem **265**:2184–2189, 1990.
14. Zaidi NF, Lagenaur CF, Abramson JJ, Pessah I, Salama G. Reactive disulfides trigger Ca^{2+} release from sarcoplasmic reticulum via an oxidation reaction. J Biol Chem **264**:21725–21736, 1989.
15. George JN, Turner RJ. Inactivation of the rabbit parotid Na/K/Cl cotransporter by N-ethylmaleimide. J Membrane Biol **112**:51–58, 1989.
16. Silva PJ, Staff J, Field J, Fine L, Forrest JN, Epstein FH. Mechanism of active chloride secretion by shark rectal gland: Role of Na-K-ATPase in chloride transport. Am J Physiol **233**:F298–F306, 1977.
17. Melvin JE, Moran A, Turner RJ. The role of HCO_3^- and Na^+/H^+ exchange in the response of rat parotid acinar cells to muscarinic stimulation. J Biol Chem **263**:19564–19569, 1988.
18. Lau KR, Elliot AC, Brown PD. Acetylcholine-induced intracellular acidosis in rabbit salivary gland acinar cells. Am J Physiol **256**:C288–C295, 1989.
19. Soltoff SP, McMillian MK, Cantley CC, Cragoe EJ, Talamo BR. Effects of muscarinic, alpha-adrenergic, and substance P agonists and ionomycin on ion transport mechanisms in the rat parotid acinar cell. The dependence of ion transport on intracellular calcium. J Gen Physiol **93**:285–319, 1989.
20. Steward MC, Seo Y, Case MR. Intracellular pH during secretion in the perfused rabbit mandibular salivary gland measured by ^{31}P NMR spectroscopy. Pflügers Arch **414**:200–207, 1989.
21. Lee SI, Turner RJ. Mechanisms of secretagogue-induced HCO_3^- and Cl^- loss from rat parotid acini. Am J Physiol **261**:G111–G118, 1991.
22. Zhang GH, Melvin JE. Regulation of cytoplasmic pH in rat

sublingual mucous acini at rest and during muscarinic stimulation. J Membrane Biol **129**:311–321, 1992.
23. Arreola J, Melvin JE, Begenisich T. Inhibition of Ca^{2+}-dependent Cl^- channels from secretory epithelial cells by low internal pH. J Membrane Biol **147**:95–104, 1995.
24. Melvin JE, Koek L, Zhang GH. A capacitative Ca^{2+} influx is required for sustained fluid secretion in sublingual mucous acini. Am J Physiol **261**:G1043–G1050, 1991.
25. Zhang GH, Arreola J, Melvin JE. Inhibition by thiocyanate of muscarinic-induced cytosolic acidification and Ca^{2+} entry in rat sublingual acini. Archs Oral Biol **40**:111–118, 1995.
26. Thomas JA, Buchabaum RN, Zimniak A, Racker E. Intracellular pH measurements in Ehrlich Ascites tumor cells utilizing spectroscopic probes generated *in situ*. Biochemistry **18**:2210–2218, 1979.
27. Roos A, Boron WF. Intracellular pH. Physiol Rev **61**:296–434, 1981.
28. Zhang GH, Melvin JE. Inhibitors of the intracellular Ca^{2+} release mechanism prevent muscarinic-induced Ca^{2+} influx in rat sublingual mucous acini. FEBS Lett **327**:1–6, 1993.
29. Zhang GH, Melvin JE. Membrane potential regulates Ca^{2+} uptake and inositol phosphate generation in rat sublingual mucous acini. Cell Calcium **14**:551–562, 1993.
30. Grynkiewicz G, Poenie M, Tsien RY. A new generation of Ca^{2+} indicators with greatly improved fluorescence properties. J Biol Chem **260**:3440–3450, 1985.
31. Merritt JE, Hallam TJ. Platelets and parotid acinar cells have different mechanisms for agonist-stimulated divalent cation entry. J Biol Chem **263**:6161–6164, 1988.
32. Batt ER, Abbott RE, Schachter D. Impermeant maleimides. Identification of an exofacial component of the human erythrocyte hexose transport mechanism. J Biol Chem **251**:7184–7194, 1976.
33. May JM. Inhibition of hexose transport in the human erythrocyte by 5,5′-dithiobis(2-nitrobenzoic acid): Role of an exofacial carrier sulfhydryl gorup. J Membrane Biol **108**:227–233, 1989.
34. VanSteveninck J, Weed RI, Rothstein A. Localization of erythrocyte membrane sulfhydryl groups essential for glucose transport. J Gen Physiol **48**:617–632, 1965.
35. Rothstein A. Sulfhydryl groups in membrane structure and function. Curr Top Membr Transp **1**:135–176, 1970.
36. Nauntofte B, Poulsen JH. Effects of Ca^{2+} and furosemide on Cl^- transport and O_2 uptake in parotid acini. Am J Physiol **251**:C175–C185, 1986.
37. Iwatsuki N, Maruyama Y, Matsumoto O, Nishiyama A. Activation of Ca^{2+}-dependent Cl^- and K^+ conductances in rat and mouse parotid acinar cells. Jpn J Physiol **35**:933–944, 1985.
38. Cook DI, Day ML, Champion MP, Young JA. Ca^{2+} not cyclic AMP mediates the fluid secretory response to isoproterenol in the rat mandibular salivary gland: Whole-cell patch-clamp studies. Pflügers Arch **413**:67–76, 1988.
39. Owen NE, Villereal ML. Effect of the intracellular Ca^{2+} antagonist TMB-8 on serum-stimulated Na^+ influx in human fibroblasts. Biochem Biophys Res Commun **109**:762–768, 1982.
40. Webb JL. *N*-Ethylmaleimide. In: Webb JL, Ed. Enzyme and Metabolic Inhibitors. New York: Academic Press, p 337, 1966.
41. Abbott RE, Schachter D. Impermeant maleimides. Oriented probes of erythrocyte membrane proteins. J Biol Chem **251**:7176–7183, 1976.